Density Functional Study of $LaFeAsO_{1-x}F_x$: A Low Carrier Density Superconductor Near Itinerant Magnetism

D. J. Singh and M.-H. Du

Materials Science and Technology Division, Oak Ridge National Laboratory, Oak Ridge, Tennessee 37831-6114, USA

(Received 4 March 2008; published 12 June 2008)

Density functional studies of 26 K superconducting LaFeAs(O,F) are reported. We find a low carrier density, high density of states, $N(E_F)$, and modest phonon frequencies relative to T_c. The high $N(E_F)$ leads to proximity to itinerant magnetism, with competing ferromagnetic and antiferromagnetic fluctuations and the balance between these controlled by the doping level. Thus LaFeAs(O,F) is in a unique class of high T_c superconductors: high $N(E_F)$ ionic metals near magnetism.

DOI: 10.1103/PhysRevLett.100.237003 PACS numbers: 74.25.Jb, 71.18.+y, 74.25.Kc, 74.70.Dd

Understanding the interplay between superconductivity and spin fluctuations especially near magnetic phases is an important challenge. The discovery of a new family of layered superconductors containing the magnetic elements Fe and Ni and critical temperatures up to $T_c = 26$ K, specifically LaOFeP ($T_c = 4$ K, and ~7 K with F doping) [1,2], LaONiP ($T_c = 3$ K) [3], and F doped LaOFeAs with $T_c = 26$ K (Ref. [4]), raises questions about the relationship between magnetism and superconductivity, the origin of the remarkably high T_c, and the chemical and structural parameters that can be used to tune the properties. Here we show that LaOFeAs is in fact close to magnetism, with competing ferromagnetic and antiferromagnetic fluctuations, with the balance controlled by doping. Furthermore, we identify La(O,F)FeAs as a nearly 2D, low carrier density metal, with modest phonon frequencies relative to T_c, and high density of states.

The crystal structure is layered with apparently distinct LaO and transition metal pnictide layers (see, e.g., Ref. [4]). Importantly, it forms with a wide range of rare earths and pnictogens, with the transition elements Mn, Fe, Co, Ni, Cu, and Ru, and additionally, related fluorides and chalcogenides are known [1–5]. It may be that there are other superconducting compositions that remain to be discovered in this family.

Our calculations were done using the local spin density approximation (LSDA) and the generalized gradient approximation (GGA) of Perdew, Burke, and Ernzerhof (PBE) [6]. We used the linearized augmented plane wave (LAPW) method with tested basis sets and zone samplings for the electronic structure [7,8]. Two independent LAPW codes were used—an in-house code and the WIEN2K package [9]. Transport properties were calculated using BOLTZTRAP [10]. The phonon dispersions were obtained in linear response via the quantum ESPRESSO code and ultrasoft pseudopotentials with a cutoff energy of 50 Ry and the PBE GGA. The codes were cross-checked by comparing band structures and zone center Raman frequencies. We used the experimental lattice parameters $a = 4.035\,52$ Å, $c = 8.7393$ Å, for LaFeAsO. The internal coordinates were determined by local density approximation (LDA) energy minimization as $z_{La} = 0.1418$ and $z_{As} = 0.6326$. The corresponding Raman modes have mixed character and frequencies of 185 and 205 cm^{-1}. The corresponding ultrasoft pseudopotential values were 181 and 203 cm^{-1}. The FeAs layers consist of a square lattice sheet of Fe coordinated by As above and below the plane to form face sharing $FeAs_4$ tetrahedra. These are squeezed along c (the As-Fe-As angles are 120.2° and 104.4°). The Fe-As distance is 2.327 Å. The Fe-Fe distance is 2.854 Å, which is short enough for direct Fe-Fe hopping to be important, while the As-As distances are 3.677 Å, across the Fe layer, and $a = 4.036$ Å, in plane.

The electronic density of states (DOS) and band structure are shown in Figs. 1 and 2. The band structure is similar to that reported for LaFePO [11]. Near the Fermi energy E_F it is well described as coming from 2D metallic sheets of Fe^{2+} ions in an ionic matrix formed by the other atoms. There is a group of 12 bands between −5.5 eV (relative to E_F) and −2.1 eV. These come from O p and As p states, with the As p contribution concentrated above −3.2 eV. These As derived bands are hybridized with the

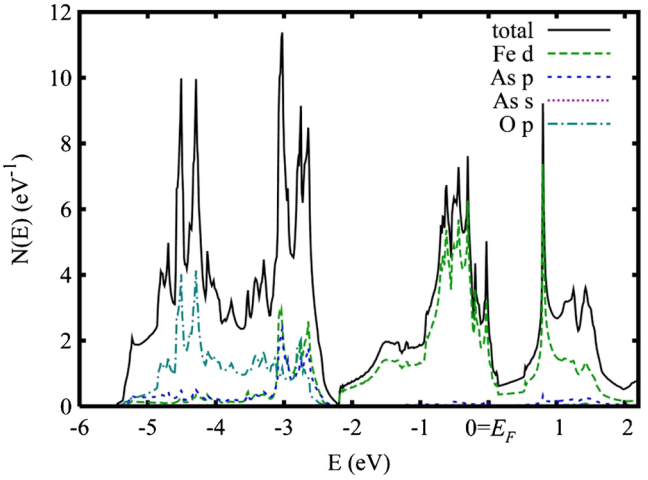

FIG. 1 (color online). LDA density of states and projections onto the LAPW spheres on a per formula unit both spins basis. Note that much of the As p character will be outside the As sphere, reducing their apparent weight.

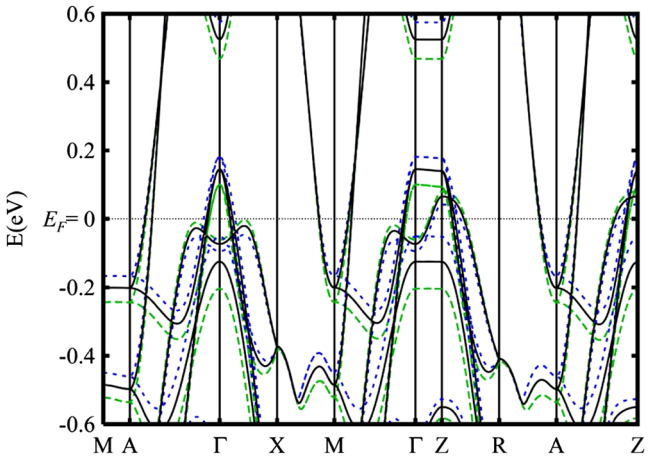

FIG. 2 (color online). Band structure of LaFeAsO around E_F showing the effect of As breathing along z by $\delta z_{\mathrm{As}} = 0.04$ (0.035 Å). The unshifted band structure is indicated by the solid black line, while the shift away (towards) the Fe is indicated by the blue dotted lines (green dashed lines).

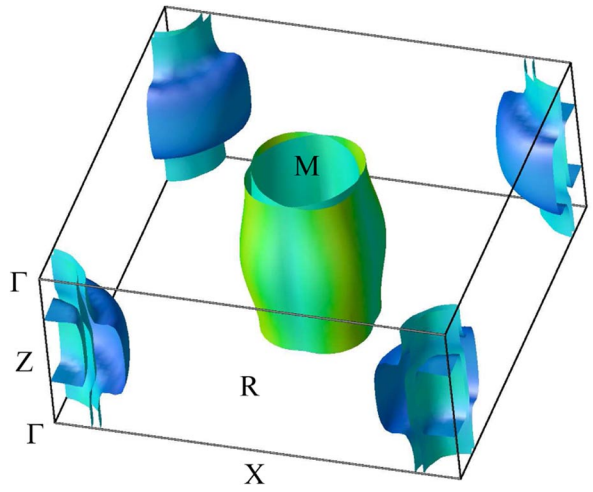

FIG. 3 (color online). LDA Fermi surface of LaFeAsO shaded by velocity [darker (blue) is low velocity]. The symmetry points are $\Gamma = (0, 0, 0)$, $Z = (0, 0, 1/2)$, $X = (1/2, 0, 0)$, $R = (1/2, 0, 1/2)$, $M = (1/2, 1/2, 0)$, $A = (1/2, 1/2, 1/2)$.

Fe d states. The Fe d states account for the bands between -2.2 and 2 eV, with La derived states occurring at higher energy. This is the ordering expected from the Pauling electronegativities: 3.44 for O, 2.18 for As, 1.83 for Fe, and 1.10 for La. While there is some hybridization between Fe and As, it is not strong and is comparable to oxides. Thus a separation of the structure into independent LaO and FeAs subunits is not justified from the point of view of electronic structure or bonding and so we write the chemical formulas in order of electronegativity. This ionic view is supported by the similarity of the Fe d derived bands of LaFePO and LaFeAsO in spite of the chemical differences between P and As. This suggests that doping mechanisms other than replacement of O by F may be effective, i.e., on the La site (e.g., by Th) or the As site (e.g., by Te or Se). This may allow stabilization of the compound with a wider range of doping levels than can be achieved using the O site, perhaps leading to higher T_c.

Fe d states would normally split into a lower lying e_g manifold and higher lying t_{2g} states in an As tetrahedral crystal field. The gap between these would be at a d electron count of 4 per Fe. However, this crystal field competes with the direct Fe-Fe interaction to yield a more complicated band structure, with no clear gap at 4 electrons per Fe. Rather, the main feature is a pseudogap at an electron count of 6. The Fermi energy for d^6 Fe^{2+} is at the pseudogap. While we do find sensitivity of the bands near E_F to the As height as shown in Fig. 2, the PBE band structure with the PBE relaxed structure is very similar to the LDA band structure, including the details of the Fermi surface.

The Fermi surface (Fig. 3) has five sheets: two high velocity electron cylinders around the zone edge M-A line, two lower velocity hole cylinders around the zone center, and an additional heavy 3D hole pocket, which intersects and anticrosses with the hole cylinders, and is centered at Z. The heavy 3D pocket is derived from Fe d_z states, which hybridize sufficiently with As p and La orbitals to yield a 3D pocket. The remaining sheets of Fermi surface are nearly 2D. The electron cylinders are associated with in-plane Fe d orbitals and have higher velocity and will make the larger contribution to the in-plane electrical conductivity, The Seebeck coefficients are positive because of the proximity to band edges in the hole bands: $S_{xx} = S_{yy} = 6.8\ \mu\mathrm{V/K}$ and $S_{zz} = 8.5\ \mu\mathrm{V/K}$, at 300 K. However, for $N(E_F)$ and other quantities that depend on the density of states, such as spin fluctuations, and electron-phonon coupling, the heavier hole pockets may be more important. Specifically, the three hole sheets together contribute 80% of $N(E_F)$ but only 31% of $N(E_F)v_x^2$. The average Fermi velocities are 0.81×10^7 cm/s (in plane) and 0.34×10^7 cm/s (c axis) for the hole sections and 2.39×10^7 cm/s (in plane) and 0.35×10^7 cm/s (c axis) for the electron sections. Including all sheets, $v_{xx} = v_{yy} = 1.30 \times 10^7$ cm/s and $v_{zz} = 0.34 \times 10^7$ cm/s. This yields a resistivity anisotropy of $\sim$15 for isotropic scattering. We note that the DOS is rapidly changing near E_F, and therefore these quantities will be quite sensitive to the electron filling, structure, and other details.

The volume enclosed by the two electron cylinders (equal to that enclosed by the hole sections) corresponds to 0.26 electrons per cell (0.13 per formula unit). E_F lies just above a peak in the DOS, which leads to a rapidly decreasing DOS with energy. This peak is associated with a van Hove singularity from the 3D hole pocket, which becomes cylindrical as E_F is lowered. The calculated value at E_F is $N(E_F) = 2.62\ \mathrm{eV}^{-1}$ per formula unit both spins. The corresponding bare susceptibility and specific heat coefficient are $\chi_0 = 8.5 \times 10^{-5}$ emu/mol and $\gamma_0 = 6.5\ \mathrm{mJ/mol\,K^2}$. Thus LaFeAsO is a low carrier concentration, high density of states superconductor. This is in contrast to the cuprates, which have high carrier concentration (near half filling with large Fermi surfaces) [12] and

lower density of states. Recent experimental data also indicate low carrier concentration [13–15]. Electron doping mainly shrinks the hole pockets, especially the 3D sheet, since these have higher mass than the electron surfaces. This leads to an increasingly 2D Fermi surface. Within Stoner theory a ferromagnetic instability occurs when $NI > 1$, with N now on a per spin basis. Since the DOS near E_F is close to pure Fe d in character it is appropriate to choose $I \sim 0.7$–0.8 eV, which would put LaFeAsO very close to a magnetic instability.

Fixed spin moment calculations were done for the LaFeAsO, LaFePO, and LaNiPO, and for LaFeAsO with O replaced by virtual atoms, $Z = 7.9$ and $Z = 8.1$ (to simulate doping) [16]. In the LDA, LaFeAsO is indeed on the border line of a ferromagnetic instability and electron doping moves away from this instability. The ground state is an itinerant ferromagnet with a moment of 0.08 μ_B/Fe. However, the small energies involved are below the precision of the calculation, so it may only be concluded that the material is on the border line of ferromagnetism. This borderline behavior, where the energy is independent of magnetization, persists up to ~0.2 μ_B/Fe. This is close to the value where the holes become fully polarized. This places stoichiometric LaFeAsO near a ferromagnetic quantum critical point.

The experimental susceptibility [4] $\chi(T)$ of undoped LaFeAsO is weakly temperature dependent between 20 and 300 K, with value $\sim 50 \times 10^{-5}$ emu/mol, and increases strongly at lower T. While the low T $\chi(0)$ is not known, even taking the higher temperature value, the implied Stoner renormalization $(1 - NI)^{-1}$ from $\chi_{\rm exp}/\chi_0$ is 6 and is probably significantly higher depending on the observed upturn below 20 K. By comparison $\chi_{\rm exp}/\chi$ is ~5 for $MgCNi_3$ [17], ~7 for Sr_2RuO_4 [18], and ~9 for Pd metal. Ferromagnetic spin fluctuations are strongly pair breaking for singlet superconductivity both in the s channel favored by electron-phonon interactions and in d channels, such as in the high-T_c cuprates. Thus such fluctuations would suppress T_c. However, it is conceivable that a sufficiently strong electron-phonon interaction, which is needed to explain the $T_c \sim 26$ K in that scenario, could overcome the pair breaking effects of ferromagnetic fluctuations as was discussed for $MgCNi_3$ [17,19]. Turning to the F doped material, which is the actual superconducting phase, $\chi_{\rm exp}$ is higher than for the stoichiometric material and increases as T is reduced over the whole temperature range, rising to $\sim 200 \times 10^{-5}$ emu/mol at T_c. This is opposite to the trends with band filling in $N(E_F)$ and the fixed spin moment curves. The simplest explanation would be in terms of secondary phases. Another explanation is that the undoped compound is magnetically ordered. There is in fact a resistivity peak at ~150 K and a minimum at ~100 K [4], but $\chi(T)$ does not show strong changes at these temperatures.

We did calculations with an antiferromagnetic arrangement of the Fe spins in the square lattice. As for ferromagnetic alignment, we find a borderline instability, with stable moments in the virtual crystal calculations at lower electron count while the proximity to antiferromagnetism is reduced with increasing electron count. We also did calculations with small fields applied to the Fe LAPW spheres in both ferromagnetic and antiferromagnetic configurations. The resulting moments, defined by the magnitude of the spin polarization in each Fe LAPW sphere, are shown in Fig. 4, along with results of similar calculations for LaNiPO and LaFePO.

While ferromagnetism is initially favored, the antiferromagnetic response becomes larger for higher fields with a crossover at an energy scale of 30 K. Thus thermal fluctuations at higher temperature and perhaps quantum fluctuations would both favor antiferromagnetic fluctuations over ferromagnetism. This nearest neighbor antiferromagnetism is related to superexchange [20]. Doping with electrons rapidly reduces the proximity to ferromagnetism. Furthermore, it should be emphasized that LaNiPO, which is also a superconductor, has much lower susceptibility for both ferromagnetic and antiferromagnetic fluctuations.

The calculated phonon dispersions and density of states of LaFeAsO are shown in Fig. 5. The acoustic modes are not strongly anisotropic. In particular, there are no soft elastic constants associated with shearing of the planes along the c axis. The Debye temperature from the acoustic mode velocities is $\Theta_D = 340$ K with an uncertainty of 10% due to sampling. Turning to the optic modes, the dispersions may be divided into two regions. Below ~300 cm^{-1} the dispersions are dominated by metal and As modes of mixed character, while the modes above ~300 cm^{-1} are strongly O derived. The phonon density of states shows three main peaks below 300 cm^{-1}. These are all of mixed metal and As character, and are a large peak centered at ~100 cm^{-1} and smaller peaks at ~170 and ~280 cm^{-1}.

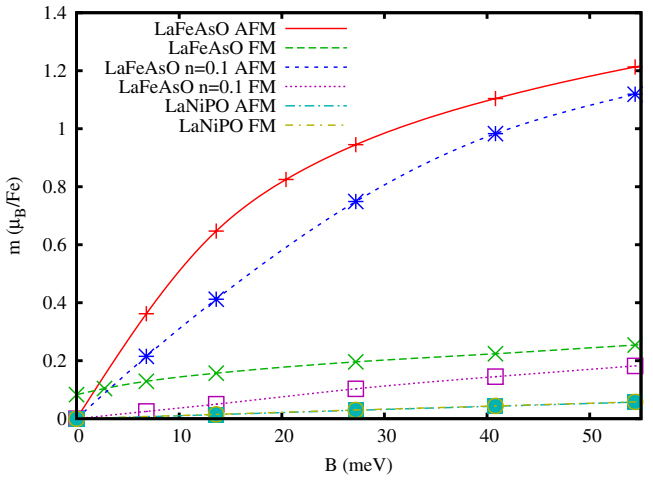

FIG. 4 (color online). Induced moments as a function of antiferromagnetic (AFM) and ferromagnetic (FM) field. The field is applied by an extra spin dependent potential $+/-B$ inside the Fe/Ni LAPW spheres.

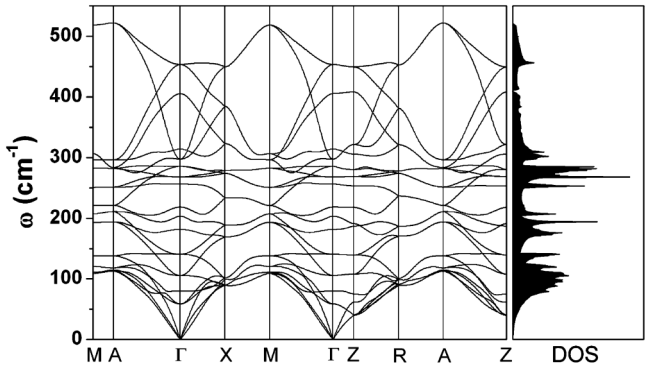

FIG. 5. Phonon dispersions and density of states of LaFeAsO.

The phosphides LaFePO and LaNiPO also superconduct, though with lower T_c. The band structures near E_F of LaFeAsO and LaFePO (Ref. [11]) are very similar. We find that LaFePO, like LaFeAsO, is on the border line of a ferromagnetic state in the LSDA. As expected from the different electron count, the electronic structure of LaNiPO is very different. Calculations yield large two-dimensional Fermi surfaces and lower $N(E_F)$. With the assumption that the origin of superconductivity is the same in the Fe and Ni compounds, spin-fluctuation mechanisms seem unlikely since these depend on a match between the **q** dependent susceptibility and the Fermi surface, requiring different coincidences for the Fe and Ni compounds. One scenario would be that there are strong electron-phonon interactions related to the layered crystal structures and the presence of high charge ionic species in proximity to metallic layers. Then ferromagnetic spin fluctuations are pair breaking and the main difference between the P and As compounds is the heavier mass of As, yielding a trend opposite to the usual isotope effect. Conversely, if the superconductivity of the Ni compound has a different origin (note the low T_c of LaNiPO), a common spin-fluctuation based mechanism for the two Fe compounds is likely. Based on the suppression in the ferromagnetic susceptibility on doping the relevant fluctuations would be antiferromagnetic in nature. In both scenarios, doping plays a key role in the Fe based compounds. Electron doping reduces $N(E_F)$, which would lower pairing strength by reducing the phase space, and at the same time strongly suppresses ferromagnetic fluctuations, which are strongly pair breaking for singlet superconductivity. Furthermore, antiferromagnetic spin fluctuations are also weakened by electron doping, which is of relevance if these are involved in the pairing. One way of distinguishing these pictures would be via doping on the Fe site, e.g., with Co or Ni. Since the electronic structure near E_F is from Fe d bands, such doping would be much more strongly scattering than doping in the O layer and would be very detrimental to non-s-wave spin fluctuation mediated superconductivity but not to s-wave superconductivity. It will be interesting to map out the similarities and differences between LaFeAsO and other superconductors with ionic metal type electronic structures, and systematically explore the relationship between spin fluctuations and superconductivity.

We are grateful for discussions with D. G. Mandrus, B. C. Sales, R. Jin, and M. Fornari and support from DOE, Division of Materials Sciences and Engineering.

[1] Y. Kamihara *et al.*, J. Am. Chem. Soc. **128**, 10012 (2006).
[2] C. Y. Liang *et al.*, Supercond. Sci. Technol. **20**, 687 (2007).
[3] T. Watanabe *et al.*, Inorg. Chem. **46**, 7719 (2007).
[4] Y. Kamihara *et al.*, J. Am. Chem. Soc. **130**, 3296 (2008).
[5] P. Quebe *et al.*, J. Alloys Compd. **302**, 70 (2000), and references therein.
[6] J. P. Perdew *et al.*, Phys. Rev. Lett. **77**, 3865 (1996).
[7] D. J. Singh and L. Nordstrom, *Planewaves, Pseudopotentials, and the LAPW Method* (Springer, Berlin, 2006), 2nd ed.
[8] LAPW sphere radii of $2.2a_0$ for La, $2.1a_0$ for Fe, $2.1a_0$ for As, and $1.6a_0$ for O were used. The final zone samplings for the density of states consisted of a $32 \times 32 \times 8$ mesh, which was then interpolated to higher density for the Fermi surface plot. The magnetic calculations were done using a $24 \times 24 \times 4$ special **k**-points mesh or better.
[9] P. Blaha *et al.*, computer code WIEN2K, TU Wien, Vienna, 2001.
[10] G. K. H. Madsen and D. J. Singh, Comput. Phys. Commun. **175**, 67 (2006).
[11] S. Lebegue, Phys. Rev. B **75**, 035110 (2007).
[12] W. E. Pickett *et al.*, Science **255**, 46 (1992).
[13] G. F. Chen, Z. Li, J. Zhou, D. Wu, J. Dong, W. Z. Hu, P. Zheng, Z. J. Chen, J. L. Luo, and N. L. Wang, arXiv:0803.0128.
[14] H. Yang, X. Zhu, L. Fang, G. Mu, and H. H. Wen, arXiv:0803.0623.
[15] R. Jin *et al.* (private communication).
[16] The virtual crystal approximation differs from the rigid band approximation as it self-consistently includes the average change in potential, but neglects randomness. It is generally valid when the scattering effect of disorder is weak, as may be expected here because O does not participate in the states near the Fermi energy, and the O ions are located far from the Fe planes.
[17] D. J. Singh and I. I. Mazin, Phys. Rev. B **64**, 140507 (2001).
[18] Y. Maeno *et al.*, Nature (London) **372**, 532 (1994).
[19] A. Y. Ignatov *et al.*, Phys. Rev. B **68**, 220504(R) (2003).
[20] The antiferromagnetism discussed here is a nearest neighbor antiferromagnetism related to superexchange. Reports following the submission of this Letter indicate that at zero doping there is a spin density wave instability at zero doping, likely at the M point, which provides an actual antiferromagnetic ground state; J. Dong *et al.*, arXiv:0803.3426; C. de la Cruz *et al.*, arXiv:0804.0795; M. A. McGuire *et al.*, arXiv:0804.0796.